ERJ Express. Published on June 11, 2008 as doi: 10.1183/09031936.00045507

Shroom expression is attenuated in pulmonary arterial hypertension

Julia Sevilla-Pérez[*], Melanie Königshoff[*], Grazyna Kwapiszewska[#], Oana V. Amarie[*], Werner Seeger[*], Norbert Weissmann[*], Ralph T. Schermuly[*], Rory E. Morty[*], and Oliver Eickelberg[*]

From the [*]Department of Medicine and [#]Department of Pathology, University of Giessen Lung Center, Justus Liebig University Giessen, Giessen, Germany

Correspondence:

Oliver Eickelberg, M.D.

University of Giessen Lung Center

Department of Medicine II phone: +49 (641) 9942300

Aulweg 123, Room 6-11 fax: +49 (641) 9942309

D-35392 Giessen email: oliver.eickelberg@innere.med.uni-giessen.de

Short title: Shroom expression in PAH

Abstract

Shroom is a PDZ domain protein involved in the regulation and maintenance of cytoskeletal architecture by binding to actin. Hypertrophy and altered actin organization of pulmonary arterial smooth muscle cells (PASMC) is a hallmark of pulmonary arterial hypertension (PAH). The aim of this study was to localise and characterise Shroom expression in the lung in experimental and idiopathic (I)PAH.

Shroom expression and localization in hypoxia-induced PAH in mice and IPAH in humans *in vivo*, as well as in primary PASMC *in vitro*, was assessed by quantitative RT-PCR, immunofluorescence, laser-assisted microdissection, and immunohistochemistry.

Shroom localised exclusively to pulmonary smooth muscle cells (both bronchial and vascular) in mouse and human lungs. *In vivo* and in primary PASMC *in vitro*, Shroom exhibited spatially similar expression with α-smooth muscle actin (α-SMA). Shroom expression was significantly reduced in the mouse model of PAH, in primary murine PASMC exposed to hypoxia, as well as in primary PASMC isolated from patients with IPAH. The ratio between Shroom and αSMA RNA expression further confirmed Shroom downregulation in both mouse and human PASMC.

In summary, Shroom localises exclusively to pulmonary smooth muscle cells. Shroom downregulation in PAH suggests a link between Shroom expression and PASMC hypertrophy in PAH.

Keywords: Actin-binding proteins, animal model, hypoxia, pulmonary arterial smooth muscle cells

Introduction

The normal pulmonary circulation represents a low-pressure, high-flow vascular system. Pulmonary arteries are characterised by a delicate tunica intima and media, which can be remodelled under disease conditions. Vascular remodelling, along with sustained vasoconstriction, leads to a decrease in the luminal area, and if these changes persist chronically, to the development of pulmonary arterial hypertension (PAH) [1, 2]. PAH is a devastating disorder characterised by sustained elevation of pulmonary arterial pressures, obstruction of small pulmonary arteries by plexiform and concentric lesions, intimal fibrosis, and medial hypertrophy [3, 4]. Abundant evidence from clinical and genetic studies suggest the involvement of the serotonin, bone morphogenetic protein (BMP), and angiopoietin systems in disease pathogenesis [4, 5]. The severity of PAH is determined, at least in part, by the degree of structural changes that occur within the wall of pulmonary arteries. Notable amongst these structural changes are extracellular matrix deposition, cell proliferation, and hypertrophy of pulmonary artery smooth muscle cells (PASMC), which represent key processes that lead to medial and/or adventitial thickening of pulmonary arteries [4, 6]. The development of PAH is therefore closely linked to enhanced PASMC activation and proliferation, which is preceded by reorganisation of the actin/myosin cytoskeleton. Activated PASMC display reduced contractility, but enhanced motility and growth [7]. Importantly, stimuli that play an essential role in PAH pathogenesis, such as serotonin, have been shown to induce reorganisation of the actin cytoskeleton [8].

The cytoskeleton is an integrated, dynamic network of three major types of protein filaments: actin fibres, intermediate filaments, and microtubules, which regulate cell motility, intracellular transport, and PASMC contraction [9]. Three actin isoforms exist in higher eukaryotes: α-actin, which is largely present in muscle cells, and β- and γ-actin, which are

also abundant in non-muscle cells. The actin pools are organised and regulated by a large number of specialised actin-binding proteins [10]. These actin-binding proteins are responsible for the stability, dynamics, higher order organisation, and subcellular distribution of the actin cytoskeleton [11]. Members of the recently-described Shroom family of proteins represent one group of such actin-binding proteins (12).

Shroom family members possess an N-terminal PDZ domain necessary for protein-protein interaction, an intermediate Apx/Shrm (AS) Domain 1 (ASD1) required for actin binding, and a C-terminally positioned AS Domain 2 (ASD2), necessary for actomyosin contraction [12]. Shroom participates in vertebrate development by regulating the recruitment and maintenance of the actomyosin network, and determines cell morphology in non-muscle cells, as initially observed in cell culture experiments [12, 13]. Furthermore, Shroom is essential for neural tube closure in both mice and frogs [12]. In the mouse, the *shrm* gene (encoding Shroom), positioned on chromosome 5, encodes two transcripts that give rise to two different putative protein products. These transcripts have been designated according to their size, *shrmL* (1986 amino acids) and *shrmS* (1808 amino acids) [12].

In the present study, we sought to investigate Shroom expression in the lung, as we hypothesised that expression levels of this actin-binding protein may be altered during the development of PAH. The expression and specific localisation of Shroom was analysed in an experimental model of PAH (hypoxia-induced PAH in mice), as well as in human IPAH samples. Shroom expression was downregulated in lung homogenates obtained from experimental animals with hypoxia-induced PAH. Importantly, Shroom was selectively expressed by pulmonary SMC in the mouse and in humans. Shroom expression was significantly downregulated in primary murine PASMC cultured under hypoxic conditions *in vitro*, as well as in PASMC cultured from the lungs of patients with IPAH, compared with PASMC cultured from healthy human lungs. We propose that Shroom may play an essential

role in the homeostasis of the SMC actin cytoskeleton. Since its expression is attenuated in SMC in PAH, restoration of normal levels and functions of actin-binding proteins, such as Shroom, in PAH may serve as an attractive option to modulate the severely altered SMC function in this disease.

Materials and methods

Animal procedures

Adult male C57Bl/6J mice (20-24 g) were obtained from Charles River WIGA GmbH (Sulzfeld, Germany). Animals were housed under controlled temperature (22 ºC) and lighting (12/12-hour light/dark cycle), and were allowed food and water *ad libitum*. All animal experiments were performed in accordance with institutional and national guidelines for the care and use of experimental animals. For hypoxic exposures, male C57Bl/6J mice were placed in a ventilated chamber system with a FiO_2 of 0.10. After 2, 7, or 21 days, mice were sacrificed by intraperitoneal injection of sodium pentobarbital, and lungs were extracted (n = 6-7 animals per condition). The lungs were either immediately snap-frozen in liquid nitrogen or harvested and processed for histological embedding and sectioning. Haemodynamic studies were performed in all study animals, as previously reported [14-16].

Human tissues

Lung tissue biopsies were obtained from seven patients with idiopathic PAH (mean age 34.5 ± 10.5 years; 4 females, 3 males) and six control subjects (organ donors, mean age 37.8 ± 14.1 years; 3 females, 3 males). None of the IPAH patients exhibited *BMPR2* mutations. Samples were either fixed in 4% (w/v) paraformaldehyde or snap-frozen in liquid nitrogen within 30 min after explantation. All investigations involving human tissues were performed in accordance with the Declaration of Helsinki. The study protocol was approved by the Ethics Committee of the Justus-Liebig-University School of Medicine (AZ 31/93). Informed consent was obtained from each subject or next-of-kin.

Laser-assisted microdissection

Microdissection was performed as described previously [17]. Briefly, cryo-sections from lung tissue were mounted on glass slides. After hemalaun staining, the sections were immersed in 70%, 96%, and 100% ethanol. Intrapulmonary arteries with a diameter of 250-500 μm were selected and microdissected under optical control using the Laser Microbeam System (Carl Zeiss Microimaging Gmbh, Bernried, Germany). Vessel profiles were isolated with sterile 30 G needle and transferred into a reaction tube containing 200 μl RNA lysis buffer [17].

Cell culture

Mouse PASMC were isolated from pulmonary arteries using the explant method, as described previously [14], and cultured in DMEM-F12 supplemented with 10% FCS (PAA Laboratories, Pasching, Austria). Only passages 3-6 were used for the experiments described herein, during which PASMC routinely exhibited typical spindle-shaped morphology and stained positive for α-SMA (Sigma-Aldrich). For hypoxia exposures, cells were placed in a chamber simulating hypoxic conditions with a water-saturated gas mixture of 1% O_2, 5% CO_2, and 94% N_2 at 37 ºC for 24 or 48 h.

RNA extraction

RNA was extracted from lung homogenates, microdissected arteries, or PASMC following the RNeasy Mini protocol (Qiagen, Hilden, Germany). Total RNA concentration was determined spectrophotometrically at 260 nm.

RT-PCR

The RNA isolated from lung homogenates or PASMC was reverse-transcribed using MMLV Reverse Transcriptase and Oligo$(dT)_{15}$ primers (Promega, Madison, WI). Semi-quantitative

RT-PCR was performed using GoTaq Flexi DNA Polymerase (Promega) in a total volume of 25 µl. The PCR products were resolved by agarose gel electrophoresis and visualised by ethidium bromide staining. Quantitative real-time RT-PCR was performed in a 7500 Fast Real-Time PCR System (Applied Biosystems, Foster City, CA). All reactions (in a final volume 25 µl) were carried out using Platinum® SYBR® Green qPCR SuperMix-UDG (Invitrogen, Carlsbad, CA). The cycling conditions were as follows: 95 °C for 6 min, followed by 45 cycles of 95 °C for 5 s, 60 °C for 5 s, and 72 °C for 30 s. Specific amplification of PCR products was confirmed by melting curve analysis and gel electrophoresis. Relative changes in gene expression were analysed using the ΔΔCt method: ΔΔCt = ΔCt hypoxia – ΔCt normoxia, and ΔCt = Ct (*shrm*) – Ct (*acta2*) or ΔCt = Ct reference gene – Ct (*shrm*). Ct denotes the cycle number where the fluorescence value is above the determined threshold. The intron-spanning primers used for semi- and quantitative RT-PCR are indicated in Table 1. The *pbgd*, *hprt*, or *gapdh*, ubiquitously as well as consistently-expressed genes, which are free of pseudogenes, were used as reference genes [18].

Immunostaining

Protein localisation was assessed using paraffin-embedded tissue sections and antibodies specifically recognising Shroom (sc-10310 (E-19), Santa Cruz Biotechnology, Santa Cruz, CA, at a dilution of 1:100) or α-smooth muscle actin (α-SMA, A5228, Sigma-Aldrich, at a dilution of 1:1000). Paraffin sections (3 µm) were mounted on poly-L-lysine-coated slides, dewaxed, and rehydrated by immersion in ethanol (100%, 95%, 70%) and phosphate-buffered saline (PBS, PAA Laboratories). After antigen retrieval, endogenous peroxidase activity was blocked with 3% H_2O_2 for 20 min. Antigens were detected according to the manufacturer's instruction (Histostain *Plus* Kit; Zymed/Invitrogen) [18].

For single cell analysis, PASMC were seeded in eight-well chamber slides, fixed, and permeabilised with methanol. Incubation with the primary antibodies described above was performed for one hour at room temperature, followed by incubation with rabbit fluorescein isothiocyanate-conjugated anti-goat (Zymed/Invitrogen; at a dilution of 1:300) or goat Texas Red-conjugated anti-mouse (Molecular Probes/Invitrogen; at a dilution of 1:400) antibodies, for Shroom and α-SMA, respectively. Cell nuclei were labelled with DAPI (Roche Diagnostics, Mannheim, Germany). Cells were visualised by fluorescent microscopy using a Leica AS-MDW micrscope (Bensheim, Germany) [14].

Statistical analysis

Values are presented as mean ± SEM. The means of indicated groups were compared using two-tailed Student's t-test, or a one-way analysis of variance (ANOVA) with Tukey's HSD *post hoc* test for studies with more than two groups. A level of $p < 0.05$ was considered statistically significant.

Results

Shroom expression and localization in hypoxia-induced pulmonary hypertension

Shroom expression was initially assessed in the mouse model of chronic hypoxia-induced pulmonary hypertension, using lung homogenates from mice maintained under normoxic (21% oxygen) or hypoxic (10% oxygen) conditions for 1, 7, or 21 days. Levels of mRNA encoding Shroom were decreased by up to 50% in the lungs of mice exposed to chronic hypoxia, as assessed by semi-quantitative RT-PCR (fig. 1a) and corresponding densitometric analysis (fig. 1b). Additionally, in order to accurately quantify the RNA expression levels of *shrm* (Shroom) and *acta2* (α-SMA) in the lung, quantitative real-time (q)RT-PCR was performed. As a positive control, we first assessed expression levels of *phosphoglycerate kinase (pgk)*, which has been described to be upregulated by hypoxia before [19]. Indeed, *pgk* mRNA levels were elevated in mice that developed elevated pulmonary artery pressures and vascular remodelling in response to hypoxia (fig. 2a). In contrast, *shrm* expression was downregulated in the lungs of these mice after a 21-day exposure to hypoxia (fig. 2a). Smooth muscle actin (*act2a*) levels remained unchanged (fig. 2a). Normalisation of *shrm* expression levels for *acta2*, which would demonstrate changes in *shrm* expression in the smooth muscle cell fraction of the lung homogenates, further confirmed that *shrm* expression was downregulated in the lungs of mice after a 1-day and 21-day exposure to hypoxia (fig. 2b).

In order to localise Shroom protein in the murine lung, immunohistochemical analyses were undertaken, which demonstrated that Shroom localised exclusively to pulmonary smooth muscle cells (SMC), surrounding both the bronchial and vascular structures (fig. 3). Immunohistochemical stainings of adjacent sections further showed that Shroom expression occurred in a spatially similar pattern with smooth muscle actin (α-SMA) staining, supporting its predominant expression in SMC (fig. 3). These observations validate our approach to

normalise *shrm* for *acta2* gene expression, to be able to explore changes in *shrm* expression in the smooth muscle fractions of lung homogenates. When comparing sections from mice subjected to chronic hypoxia with those from normoxic animals, we noted an increase in α-SMA staining, as expected, but a decrease in Shroom staining in the SMC (fig. 3), which are consistent with our data generated by semi-quantitative RT-PCR and qRT-PCR analyses of whole lung homogenates (figs 1 and 2).

Next, laser-assisted microdissection was performed to specifically isolate RNA from intrapulmonary arteries with a diameter of 250-500 μm from mice maintained under normoxic or hypoxic conditions, since the PASMC was the cell-type with the highest *shrm* expression *in vivo* (fig. 4a). The *shrm* expression levels were generally stable in these samples (although a small but significant increase was observed after a 21-day hypoxia exposure), as assessed by qRT-PCR (fig. 4b). In contrast, *acta2* mRNA expression was significantly elevated after 21 days of hypoxia (fig. 4b). As such, normalisation of *shrm* mRNA expression for *acta2* mRNA expression clearly demonstrated a pronounced down-regulation of *shrm* in the smooth muscle layer of intrapulmonary arteries (fig. 4c).

Shroom expression and regulation by hypoxia in primary PASMC

We then determined *shrm* mRNA expression levels in PASMC maintained under normoxic or hypoxic conditions. The *shrm* expression was significantly downregulated under low oxygen conditions, as assessed by semi-quantitative RT-PCR (fig. 5a) and qRT-PCR (fig. 5b), using RNA isolated from PASMC maintained under normoxic (21% oxygen) or hypoxic (1% oxygen) conditions for 24 or 48 h (fig. 5a, b). The *pgk* expression levels again served as a positive control for hypoxia-induced effects (fig. 5b) [19].

Given the apparent regulation of *shrm* expression by hypoxia, we screened the promoter and enhancer regions of the murine *shrm* gene for the presence of putative hypoxia-inducible

response elements (HRE) at a distance of 5,000 base pairs upstream and downstream of the coding region. These HRE are of particular interest, as they indicate regulation of mRNA expression by hypoxia-inducible factor (HIF)-1 [19]. An automated computational analysis using the gene prediction method was employed to detect the consensus HRE [ACGTGS, S being either G or C] [20]. Interestingly, four HRE were detected in the *shrm* promoter and enhancer, located at positions -1573 and +1792 of the sense strand and at -1650 and +641 of the antisense strand (fig. 5c), indicating that HIF-1 may indeed be involved in negative regulation of *shrm* expression under hypoxic conditions.

Immunofluorescence analysis of murine primary PASMC maintained under normoxic conditions illustrated a cytoplasmic localisation pattern for Shroom, and confirmed its co-localisation with α-SMA using double immunofluorescence (fig. 5d).

Shroom expression and localisation in human lungs

Shroom localisation was then assessed in control human lungs from healthy transplant donors, or lungs obtained from IPAH patients (none of which exhibited exonic *BMPR2* mutations). In the human lung, Shroom protein staining was observed predominantly in PASMC, with a lower intensity in bronchial SMC (fig. 6), suggesting a similar staining pattern to mouse lungs (compare figs 6 and 3). Staining was most intense within the tunica media of pulmonary arteries. Furthermore, Shroom exhibited a spatially similar expression pattern with α-SMA, supporting its predominant expression in SMC (fig. 6). Shroom protein was also detected in PASMC of remodelled pulmonary arteries in IPAH samples, but only weakly expressed in PASMC within plexiform lesions (fig. 6e and f, respectively).

Levels of mRNA encoding *shrm1* and *shrm3*, as well as *acta2* were then assessed in homogenates obtained from healthy human lungs or lungs from IPAH patients (fig. 7). Both *shrm1* and *acta2* mRNA levels were upregulated in lung homogenates of IPAH patients

compared with homogenates from healthy control lungs, while *shrm3* levels remained unchanged (fig. 7a). Normalisation of *shrm1* for *acta2* mRNA levels suggested that PASMC-specific changes in *shrm1* expression were not evident comparing lung homogenates from IPAH patients versus healthy donor controls (fig. 7b). When PASMC were cultured from lungs of healthy donors or patients with IPAH, no absolute changes in *shrm1* mRNA expression, but a pronounced increase in *acta2* mRNA expression were observed. Normalisation of *shrm1* for *acta2* mRNA levels in cultured PASMC, however, clearly demonstrated a downregulation of *shrm1* expression in PASMC from IPAH patients versus healthy donors.

Discussion

The novel observations reported within the present study are as follows: 1. For the first time, the presence of the actin-binding protein Shroom in mouse and human lungs was demonstrated. 2. Shroom was demonstrated to be a smooth muscle-specific protein in mouse and human lungs, and its expression was attenuated during the development of experimental PAH in the mouse. 3. Shroom was localised to the cytoplasm, along with α-SMA, in mouse PASMC. 4. While α-SMA expression increased in the disease state, Shroom expression relative to α-SMA was maintained or downregulated in PASMC in both the human disease and the mouse model of hypoxia-induced PAH.

In order to begin to decipher the role of Shroom in the lung vasculature, a mouse model of PAH was employed, where elevated pulmonary artery pressures and vascular remodelling was induced by chronic exposure to normobaric hypoxia. In this model, analysis of RNA derived from lung homogenates revealed a decreased expression of *shrm*, suggesting a potential role during disease development. Moreover, Shroom protein staining was less pronounced in PAH-induced sections compared with controls, and thus confirmed these results obtained at the mRNA level. *In vitro* data derived from PASMC further corroborated the observed downregulation of *shrm* expression by hypoxia, together suggesting that Shroom expression was attenuated during the development of PAH. Given that SMC de-differentiation and subsequent activation is a key pathophysiological parameter during the development PAH, it is reasonable to speculate that persistent Shroom expression may be required for maintenance of the quiescent SMC phenotype. It is presently unclear, however, whether attenuation of Shroom expression is an epiphenomenon, or is the cause of SMC de-differentiation and activation.

The *shroom* gene family currently consists of four members: *shroom1* (also called APXL2 or KIAA1960), *shroom2* (also called APXL, DKFZp781J074, FLJ39277, or HSAPXL), *shroom3* (formerly Shroom, but also called APXL3, KIAA1481, or MSTP013), and *shroom4* (also called RP11-119E20.1, KIAA1202), in line with a recently proposed new nomenclature [21] and the updated human genome resources database at the NCBI (http://www.ncbi.nlm.nih.gov/projects/genome/guide/human). These four members can be distinguished by several structural differences: while the PDZ and ASD1 domains are present in all members of the family, the ASD2 domain is absent in Shroom4 [12, 22]. Detailed future investigations into the spatiotemporal, but also species-specific expression pattern of all Shroom family members are required to fully investigate their role in smooth muscle cell hypertrophy in disease, as suggested herein. Of all these members, only Shroom4 has been described before to be expressed in the murine and human lung [22, 23]. Thus far, the other Shroom members have been localised in neural epithelial cells [12] and fibroblasts [13].

In light of these reports, the intense Shroom staining in rodent and human lung SMC was surprising, as it has not been previously described. What could be the possible functions of Shroom in SMC? Considering that Shroom is an actin-binding protein, which directly regulates reorganisation of the actin cytoskeleton upon cell de-differentiation and/or transformation, it is reasonable to assume that Shroom controls the actin cytoskeleton in SMC. The SMC is the primary cell type that expresses α-SMA in the lung, along with myofibroblasts under disease conditions, such as pulmonary fibrosis. Therefore, Shroom may control the cytoskeleton of the quiescent SMC under normal conditions, a regulatory function that is lost upon decreased expression of Shroom in vascular disorders such as PAH.

A large number of animal models have been utilised to study the pathogenesis of PAH, including the mouse model of chronic hypoxia-induced PAH, where muscularisation occurs in distal arterioles, with subsequent increases in right ventricular mass and pressure [24].

These processes are preceded by select alterations in the gene expression profile of cells within the vascular wall, in particular PASMC and adventitial fibroblasts [6, 25]. Particularly relevant to hypoxia-induced effects are the regulatory HRE regions in the promoter and enhancer sequences of hypoxia-regulated genes. While a large number of reports have thus far demonstrated that increased HIF-1-activity can lead to increased gene transcription, only few reports have reported the inhibition of gene transcription via HRE sites [26, 27]. As such, the four putative HRE sites found in the murine *shrm* promoter and enhancer may provide important clues for our understanding of HIF-mediated inhibition of gene transcription in response to hypoxia. In this respect, future investigations deciphering the functional contribution of sequences that are immediately adjacent to these HRE sites are required to delineate any possible regulatory sequences mediating inhibition of gene transcription in the context of hypoxia.

Major agents promote smooth muscle cell migration like endothelin-1 and chemokines such as CCL2 (MCP-1) and CX3CL1 (fractalkine) [28]. These ligands induce actin polymerisation in the cell, when bound to the corresponding chemokine receptors, and thus influence cell migration. Further study on the influence of these ligands on Shroom localisation and expression may highlight a possible therapeutic benefit of targeting Shroom or other cytoskeletal proteins in the context if IPAH. The data presented in this study also demonstrate that Shroom is expressed in airway smooth muscle cells, as well as in vascular smooth muscle cells. This observation may be relevant to diseases that are characterised by airway smooth muscle hypertrophy, such as bronchial asthma [29], in which Shroom, by virtue of its regulation of smooth muscle homeostasis, may also play a pathogenic role.

In both whole lung homogenates, and in cultured human PASMC from patients with IPAH, it is noteworthy that the effects of standard therapies for PAH (endothelin receptor antagonists, type 5 phosphodiesterase inhibitors and prostacyclin derivatives) on Shroom expression have

not been fully investigated due to the variety of treatments available. Therefore, it remains possible that pharmacological interventions in the patient population may also have influenced *shrm* RNA levels assessed in this study. We were initially surprised by the apparent discrepancy of the results documenting *shrm* expression levels in whole lung homogenates from mouse and human samples. While *shrm* expression was decreased in mouse lungs of chronic-hypoxia-induced PAH (fig. 2a), we did not observe this difference in human lungs from IPAH patients (fig. 7a). This could be explained as follows: First, as outlined above, the nomenclature of the *shrm* genes has recently evolved, and novel family members are still discovered. A close comparison of mouse and human *shrm* genes may therefore unravel novel homologues in the future, which then warrant detailed investigations in diseases associated with smooth muscle cell hypertrophy. Second, as the IPAH patients investigated herein presented with late-stage PAH, compensatory mechanisms in the human disease may have accounted for reactive changes in *shrm* expression, which were not operative in the short-term mouse model.

In conclusion, we report a novel protein, Shroom, that is possibly involved in PAH pathogenesis. While recent data has implied the bone morphogenetic protein receptor (BMPR)-II and activin-like kinase (ALK)-1 in familiar cases of PAH [30, 31], as well as angiopoietin-1, TIE2, and serotonin in all forms of PAH [32], the precise molecular mechanisms that lead to the evolution of PAH still remain elusive. Despite this, the SMC has emerged as a key cell-type that causally contributes to the increased vascular resistance in PAH. As such, the analysis of PASMC hypertrophy under disease conditions represents a valuable tool to investigate novel approaches to disease pathogenesis. Since the maintenance of cytoskeletal actin is crucial for cell shape, intracellular trafficking of compartmentalized cellular components, SMC contraction, and thus quiescence [7], we postulate that alteration to the actin organisation, possibly due to the absence of Shroom, leads to uncontrolled PASMC

hypertrophy and finally, the development of PAH. Clearly, selective and specific modification of PASMC hypertrophy in PAH may present as a valuable therapeutic tool in future investigations.

Acknowledgments

We are indebted to Sai Krishnaveni Manda for critical reading of this manuscript and the MBML class of 2007 for invaluable discussions.

References

1. Gaine SP, Rubin LJ. Primary pulmonary hypertension. *Lancet* 1998: 352(9129): 719-725.
2. Humbert M, Sitbon O, Simonneau G. Treatment of pulmonary arterial hypertension. *N Engl J Med* 2004: 351(14): 1425-1436.
3. Runo JR, Loyd JE. Primary pulmonary hypertension. *Lancet* 2003: 361(9368): 1533-1544.
4. Humbert M, Morrell NW, Archer SL, Stenmark KR, MacLean MR, Lang IM, Christman BW, Weir EK, Eickelberg O, Voelkel NF, Rabinovitch M. Cellular and molecular pathobiology of pulmonary arterial hypertension. *J Am Coll Cardiol* 2004: 43(12 Suppl S): 13S-24S.
5. Eickelberg O, Yeager ME, Grimminger F. The tantalizing triplet of pulmonary hypertension-BMP receptors, serotonin receptors, and angiopoietins. *Cardiovasc Res* 2003: 60(3): 465-467.
6. Stenmark KR, Fagan KA, Frid MG. Hypoxia-induced pulmonary vascular remodeling: cellular and molecular mechanisms. *Circ Res* 2006: 99(7): 675-691.
7. Solway J, Forsythe SM, Halayko AJ, Vieira JE, Hershenson MB, Camoretti-Mercado B. Transcriptional regulation of smooth muscle contractile apparatus expression. *Am J Respir Crit Care Med* 1998: 158(5 Pt 3): S100-108.
8. Day RM, Agyeman AS, Segel MJ, Chevere RD, Angelosanto JM, Suzuki YJ, Fanburg BL. Serotonin induces pulmonary artery smooth muscle cell migration. *Biochem Pharmacol* 2006: 71(3): 386-397.
9. Schmidt A, Hall MN. Signaling to the actin cytoskeleton. *Annu Rev Cell Dev Biol* 1998: 14: 305-338.

10. Palmgren S, Vartiainen M, Lappalainen P. Twinfilin, a molecular mailman for actin monomers. *J Cell Sci* 2002: 115(Pt 5): 881-886.

11. Pollard TD, Blanchoin L, Mullins RD. Molecular mechanisms controlling actin filament dynamics in nonmuscle cells. *Annu Rev Biophys Biomol Struct* 2000: 29: 545-576.

12. Hildebrand JD, Soriano P. Shroom, a PDZ domain-containing actin-binding protein, is required for neural tube morphogenesis in mice. *Cell* 1999: 99(5): 485-497.

13. Dietz ML, Bernaciak TM, Vendetti F, Kielec JM, Hildebrand JD. Differential actin-dependent localization modulates the evolutionarily conserved activity of Shroom family proteins. *J Biol Chem* 2006: 281(29): 20542-20554.

14. Morty RE, Nejman B, Kwapiszewska G, Hecker M, Zakrzewicz A, Kouri FM, Peters DM, Dumitrascu R, Seeger W, Knaus P, Schermuly RT, Eickelberg O. Dysregulated Bone Morphogenetic Protein Signaling in Monocrotaline-Induced Pulmonary Arterial Hypertension. *Arterioscler Thromb Vasc Biol* 2007: 27(5): 1072-1078.

15. Zakrzewicz A, Kouri FM, Nejman B, Kwapiszewska G, Hecker M, Sandu R, Dony E, Seeger W, Schermuly RT, Eickelberg O, Morty RE. The TGF-{beta}/Smad2,3 signalling axis is impaired in experimental pulmonary hypertension. *Eur Respir J* 2007: 29(6): 1094-1104.

16. Dumitrascu R, Weissmann N, Ghofrani HA, Dony E, Beuerlein K, Schmidt H, Stasch JP, Gnoth MJ, Seeger W, Grimminger F, Schermuly RT. Activation of soluble guanylate cyclase reverses experimental pulmonary hypertension and vascular remodeling. *Circulation* 2006: 113(2): 286-295.

17. Fink L, Seeger W, Ermert L, Hanze J, Stahl U, Grimminger F, Kummer W, Bohle RM. Real-time quantitative RT-PCR after laser-assisted cell picking. *Nat Med* 1998: 4(11): 1329-1333.

18. Alejandre-Alcazar MA, Kwapiszewska G, Reiss I, Amarie OV, Marsh LM, Sevilla-Perez J, Wygrecka M, Eul B, Kobrich S, Hesse M, Schermuly RT, Seeger W, Eickelberg O, Morty RE. Hyperoxia modulates TGF-beta/BMP signaling in a mouse model of bronchopulmonary dysplasia. *Am J Physiol Lung Cell Mol Physiol* 2007: 292(2): L537-549.

19. Semenza GL. Regulation of physiological responses to continuous and intermittent hypoxia by hypoxia-inducible factor 1. *Exp Physiol* 2006: 91(5): 803-806.

20. Kwapiszewska G, Wilhelm J, Wolff S, Laumanns I, Koenig IR, Ziegler A, Seeger W, Bohle RM, Weissmann N, Fink L. Expression profiling of laser-microdissected intrapulmonary arteries in hypoxia-induced pulmonary hypertension. *Respir Res* 2005: 6: 109.

21. Hagens O, Ballabio A, Kalscheuer V, Kraehenbuhl JP, Schiaffino MV, Smith P, Staub O, Hildebrand J, Wallingford JB. A new standard nomenclature for proteins related to Apx and Shroom. *BMC Cell Biol* 2006: 7: 18.

22. Yoder M, Hildebrand JD. Shroom4 (Kiaa1202) is an actin-associated protein implicated in cytoskeletal organization. *Cell Motil Cytoskeleton* 2007: 64(1): 49-63.

23. Hagens O, Dubos A, Abidi F, Barbi G, Van Zutven L, Hoeltzenbein M, Tommerup N, Moraine C, Fryns JP, Chelly J, van Bokhoven H, Gecz J, Dollfus H, Ropers HH, Schwartz CE, de Cassia Stocco Dos Santos R, Kalscheuer V, Hanauer A. Disruptions of the novel KIAA1202 gene are associated with X-linked mental retardation. *Hum Genet* 2006: 118(5): 578-590.

24. Weissmann N, Akkayagil E, Quanz K, Schermuly RT, Ghofrani HA, Fink L, Hanze J, Rose F, Seeger W, Grimminger F. Basic features of hypoxic pulmonary vasoconstriction in mice. *Respir Physiol Neurobiol* 2004: 139(2): 191-202.

25. Stenmark KR, Frid M, Nemenoff R, Dempsey EC, Das M. Hypoxia induces cell-specific changes in gene expression in vascular wall cells: implications for pulmonary hypertension. *Adv Exp Med Biol* 1999: 474: 231-258.

26. Erler JT, Cawthorne CJ, Williams KJ, Koritzinsky M, Wouters BG, Wilson C, Miller C, Demonacos C, Stratford IJ, Dive C. Hypoxia-mediated down-regulation of Bid and Bax in tumors occurs via hypoxia-inducible factor 1-dependent and -independent mechanisms and contributes to drug resistance. *Mol Cell Biol* 2004: 24(7): 2875-2889.

27. Narravula S, Colgan SP. Hypoxia-inducible factor 1-mediated inhibition of peroxisome proliferator-activated receptor alpha expression during hypoxia. *J Immunol* 2001: 166(12): 7543-7548.

28. Perros F, Dorfmuller P, Souza R, Durand-Gasselin I, Godot V, Capel F, Adnot S, Eddahibi S, Mazmanian M, Fadel E, Herve P, Simonneau G, Emilie D, Humbert M. Fractalkine-induced smooth muscle cell proliferation in pulmonary hypertension. *Eur Respir J* 2007: 29(5): 937-943.

29. Bentley JK, Hershenson MB. Airway smooth muscle growth in asthma: proliferation, hypertrophy, and migration. *Proc Am Thorac Soc* 2008: 5(1): 89-96.

30. Machado RD, Aldred MA, James V, Harrison RE, Patel B, Schwalbe EC, Gruenig E, Janssen B, Koehler R, Seeger W, Eickelberg O, Olschewski H, Elliott CG, Glissmeyer E, Carlquist J, Kim M, Torbicki A, Fijalkowska A, Szewczyk G, Parma J, Abramowicz MJ, Galie N, Morisaki H, Kyotani S, Nakanishi N, Morisaki T, Humbert M, Simonneau G, Sitbon O, Soubrier F, Coulet F, Morrell NW, Trembath RC. Mutations of the TGF-beta type II receptor BMPR2 in pulmonary arterial hypertension. *Hum Mutat* 2006: 27(2): 121-132.

31. Morrell NW. Pulmonary hypertension due to BMPR2 mutation: a new paradigm for tissue remodeling? *Proc Am Thorac Soc* 2006: 3(8): 680-686.

32. Sullivan CC, Du L, Chu D, Cho AJ, Kido M, Wolf PL, Jamieson SW, Thistlethwaite PA. Induction of pulmonary hypertension by an angiopoietin 1/TIE2/serotonin pathway. *Proc Natl Acad Sci U S A* 2003: 100(21): 12331-12336.

Figure Legends

FIGURE 1. Shroom mRNA expression in mouse lung homogenates. a) *shrm* was expressed in lungs from mice maintained under normoxic conditions. The *shrm* expression was downregulated in the lungs of mice exposed to chronic hypoxia for up to three weeks, as assessed by semi-quantitative RT-PCR. The *pbgd* gene was used as internal loading control. Positive control samples (pos.) contained commercial total RNA, negative control samples (neg.) omitted reverse transcriptase. b) Bar graph representing densitometric analysis of the gene expression ratio *shrm*/*pbgd*. OD, optical density of the amplicon assessed by densitometry. Data represent the average values obtained from three mice per condition, and are representative of the same trends observed with at least six other mice per condition. *, $p<0.05$.

Figure 1

a)

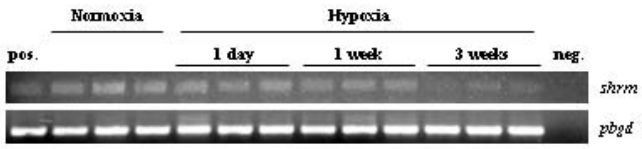

b)

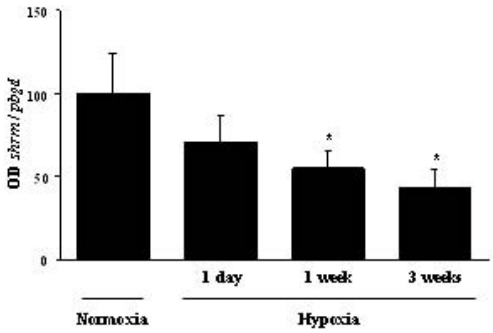

FIGURE 2. Quantitative real-time RT-PCR of *shrm* expression in mouse lung homogenates. a) The mRNA levels of phosphoglycerate kinase (*pgk*), *shrm*, or α-smooth muscle cell actin (*act2a*) were assessed in the lungs of mice exposed to normoxia or hypoxia for the indicated time. b) A normalisation of *shrm* for *act2a* gene expression, obtained from the data presented in (a). Data represent the average values obtained from three mice per condition, and are representative of the same trends observed with at least six other mice per condition. *, $p<0.05$.

Figure 2

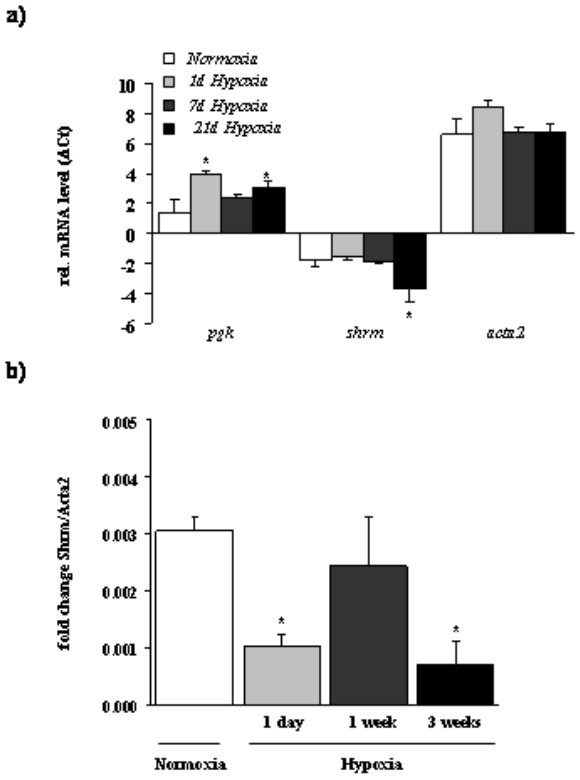

FIGURE 3. Shroom protein localisation in the mouse lung. Representative serial immunohistochemical sections illustrate a similar spatial expression of Shroom (*upper* row) and α-SMA (*lower* row) in smooth muscle cells, both in low (× 10; left panels; scale bars =

200 µm) and high (× 40; right panels; scale bars = 50 µm) magnification. a, c, e, g) Staining of normoxic mouse lungs (21% oxygen, 3 weeks); b, d, f, h) Staining of hypoxic mouse lungs (10% oxygen, 3 weeks). Images are representative for three mice per condition.

Figure 3

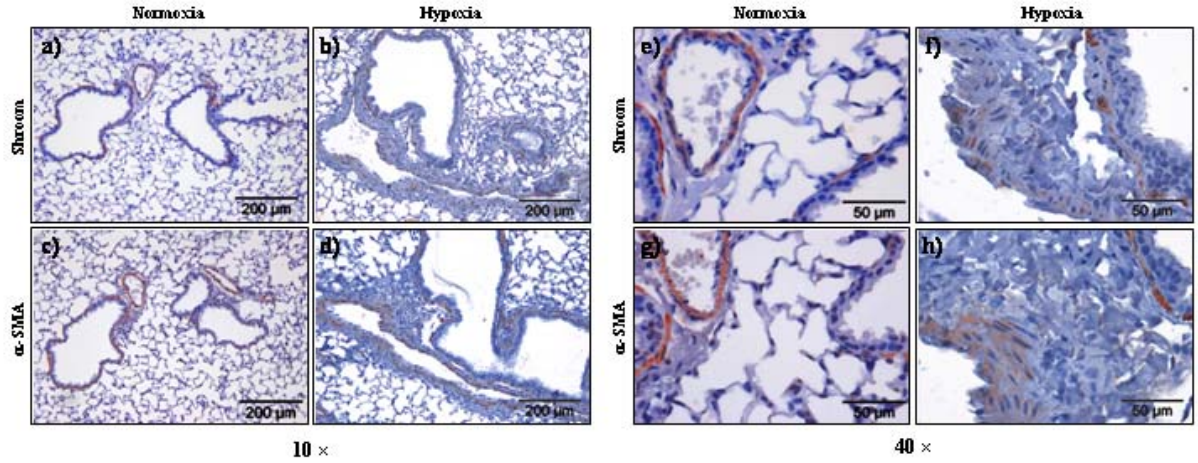

FIGURE 4. Shroom expression in microdissected intrapulmonary arteries. a) Representation of laser-assisted microdissection of small arteries. b) The *shrm* and *acta2* mRNA expression levels in microdissected intrapulmonary arteries from mice maintained under normoxic or hypoxic conditions for 1, 7, and 21 days is represented by ΔCt values. c) A normalisation of *shrm* for *act2a* gene expression, calculated from the data presented in b). *, $p<0.05$.

Figure 4

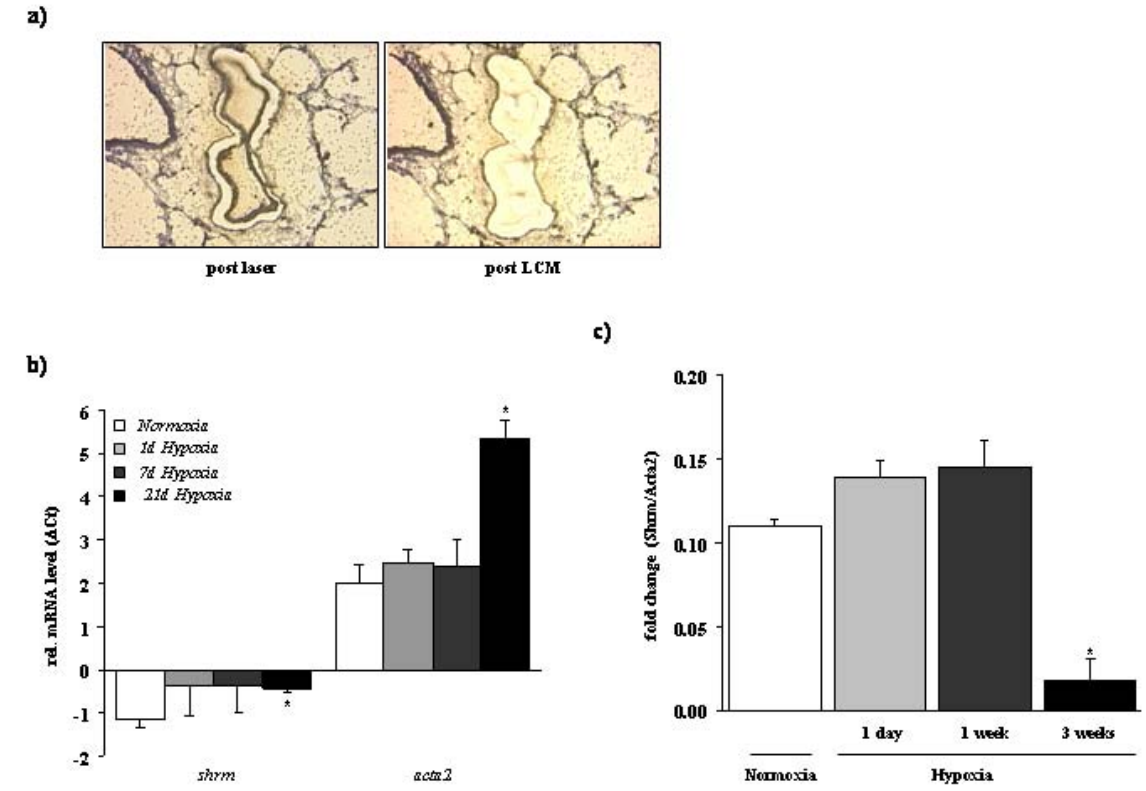

FIGURE 5. Shroom expression and regulation in mouse primary PASMC. The *shrm* mRNA expression was assessed by semi-quantitative (a) and qRT-PCR (b). An attenuation of *shrm* expression was observed in PASMC cultured under hypoxic conditions (1% oxygen) for 24 and 48 h. The *pbgd* expression was used as internal loading control, while *pgk* gene expression served as positive control for hypoxic conditions. c) Schematic illustration of the hypoxia-responsive elements (HRE) in the *shrm* promoter and enhancer regions. d) Immunofluorescence analysis of primary mouse PASMC demonstrates a cytoplasmic pattern for Shroom and α-SMA, the merged picture demonstrated co-localisation of both proteins in PASMC. *, $p<0.05$.

Figure 5

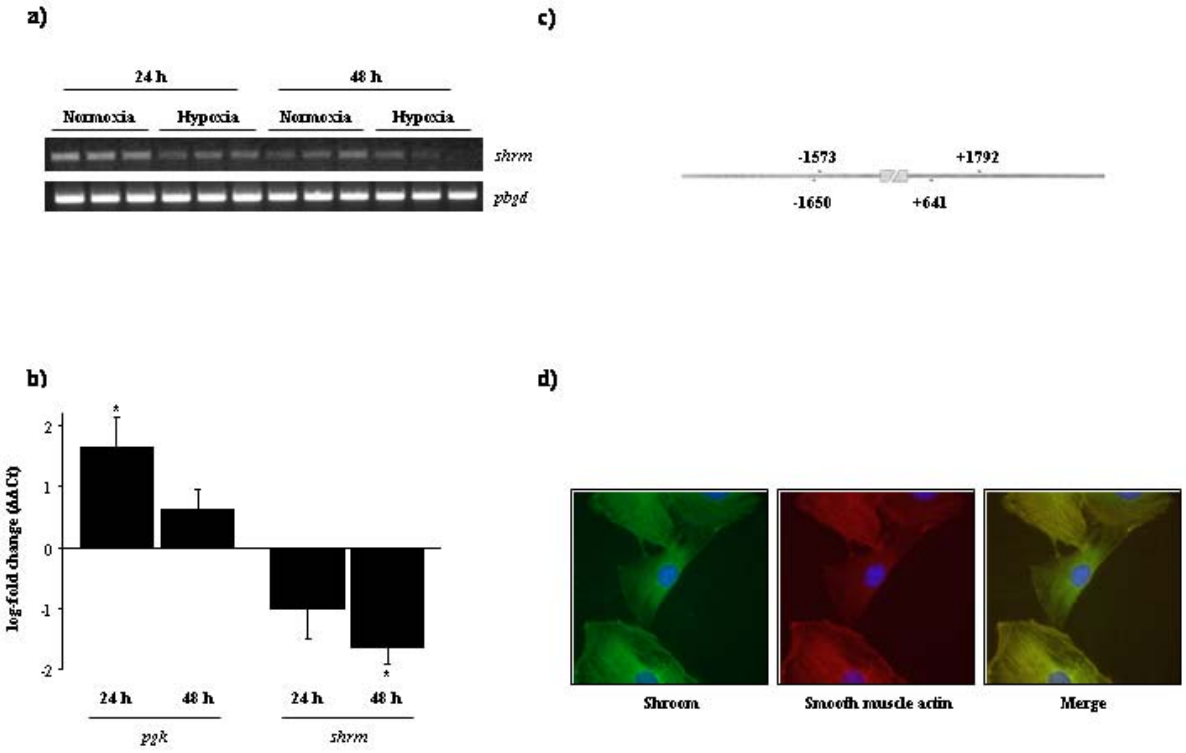

FIGURE 6. Shroom protein localisation in the human lung. Representative serial immunohistochemical sections illustrate a similar spatial expression of Shroom (*upper* row) and α-SMA (*lower* row) in smooth muscle cells, at both low (a, c, e, g, × 10; scale bars = 200 μm) or high (b, d, × 40; scale bars = 50 μm; f, h, × 20; scale bars = 100 μm) magnification. a - d) Staining of normal human lungs (transplant donors); e - h) Staining of IPAH lungs; f, g) Stainings in and around a plexiform lesion derived from an IPAH patient with no detectable *bmpr2* mutations.

Figure 6

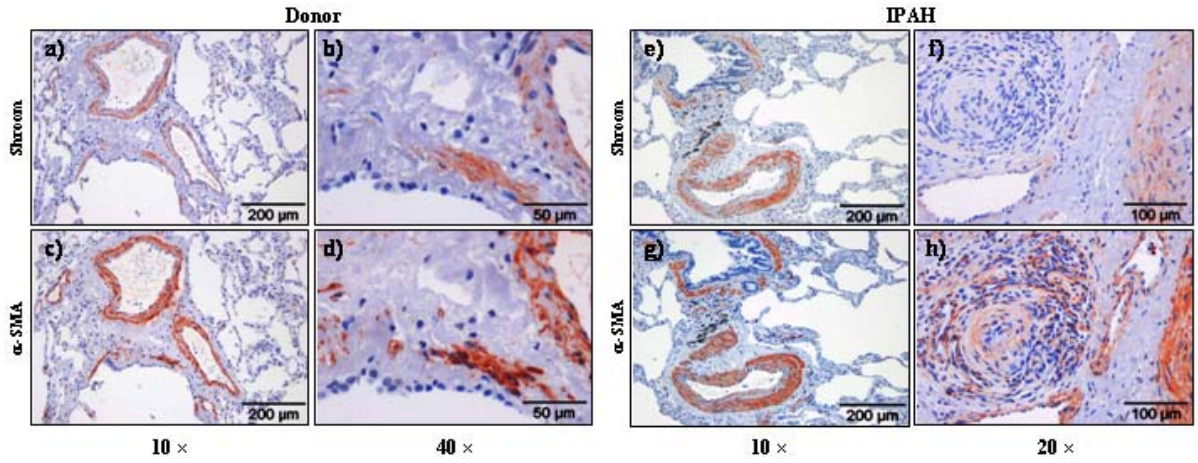

FIGURE 7. Shroom gene expression in the human lung. a) Expression levels of *shrm1*, *shrm3,* or *acta2* in lungs from healthy human donors or from IPAH patients, as depicted. b) The expression ratio *shrm*/*acta2* in control and diseased lungs is represented, calculated from the data presented in (a). *, $p<0.05$.

Figure 7

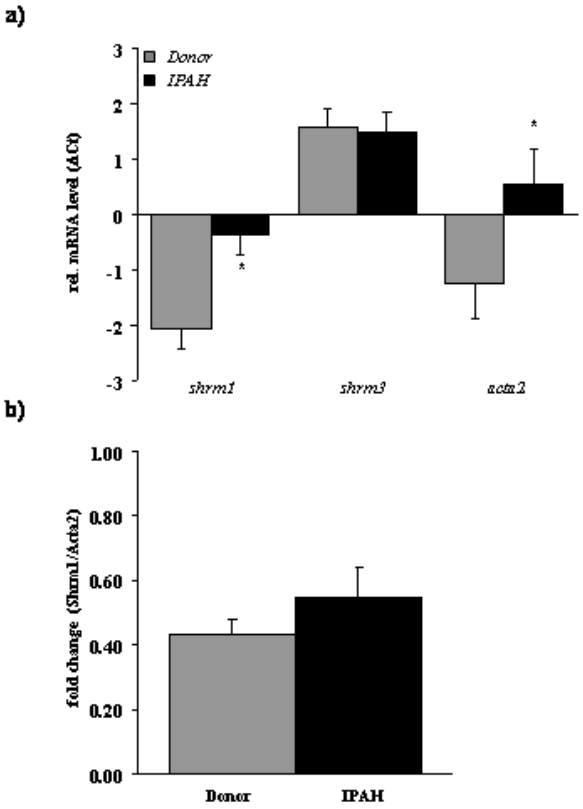

FIGURE 8. Shroom gene expression in primary PASMC cultured from donor or IPAH lungs. a) Expression levels of *shrm1* and *acta2* in pulmonary artery smooth muscle cells cultured from the lungs from healthy human donors and from IPAH patients are depicted. b) the ratios between *shrm*/*acta2* in control and diseased lungs were derived from the data presented in (a).

Figure 8

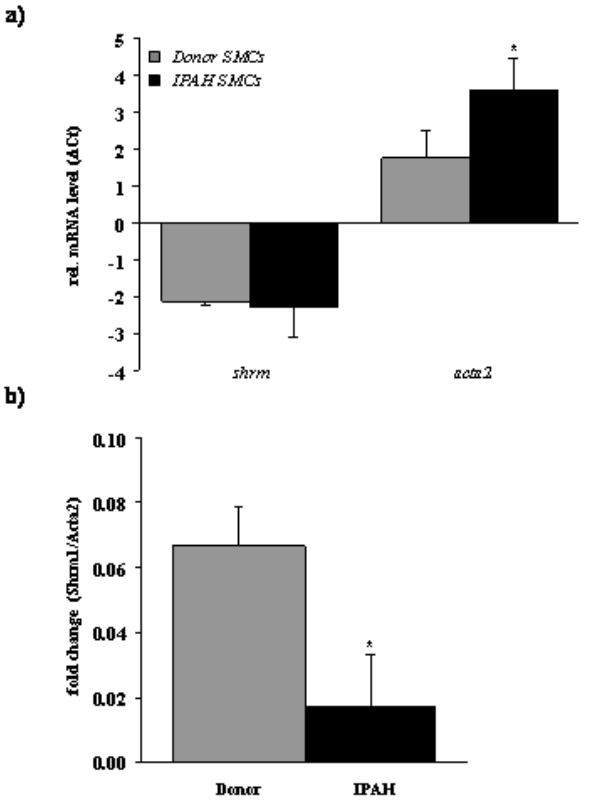
a)
Donor SMCs
IPAH SMCs
rel. mRNA level (ΔCt)
5
4
3
2
1
0
-1
-2
-3
-4
shrm
acta2
*
b)
fold change (Shrm1/Acta2)
0.10
0.08
0.06
0.04
0.02
0.00
Donor
IPAH
*

Tables

Table 1. Sequences of forward and reverse primers used for semi-quantitative and quantitative real-time RT-PCR.

Gene name	**Forward primer 5´-3´**	**Reverse primer 5´-3´**	**GenBank Accesion Nr.**
mouse *acta2*	GCTGGTGATGATGCTCCCA	GCCCATTCCAACCATTACTCC	NM_007392
mouse *pbgd*	GGTACAAGGCTTTCAGCATCGC	ATGTCCGGTAACGGCGGC	NM_013551
mouse *pgk1*	TGGGACTGTCATCCTGCTGG	GAGGCTCGGAAAGCATCAAT	NM_008828
mouse *shrm*	ACTGTCCAGGCTGTTCCTCAA	CAGCCAGCCGGTTTGGT	NM_027917
human *acta2*	CGAGATCTCACTGACTACCTCATGA	AGAGCTACATAACACAGTTTCTCCTTGA	NM_001613
human *shrm1*	AGGCGAAGTCTTGGGTTCCT	TGAGGCAAGAACCTGGAAAGTT	NM_133456
human *shrm3*	TGGATCTAGGTCACTCAGTTGTTCA	AGGAACGGAGGAATCACCAA	NM_020859
human *hprt*	AAGGACCCCACGAAGTGTTG	GGGTTTGTATTTTGCTTTTCC	NM_000194